

APPLICATION OF THE BRAGG GRATING OPTICAL SENSORS AND EDDY CURRENT METHOD FOR THE NON DESTRUCTIVE TESTING OF BONDED COMPOSITE REPAIRS

G. Tsamasphyros^a, G. Kanderakis^a, P. Vouthounis^b, I. Prassianakis^a

^aThe National Technical University of Athens, Faculty of Applied Sciences, Dept. of Mechanics-Lab. of Strength Materials, Zographou Campus, Theocaris Bld., GR-0157 73, Athens, Greece

^bTechnological Educational Inst., Dept of Civil Works Technology, Ag. Spyridonos Str., 12210 Egaleo-Athens, Greece

Abstract: The repair technology of cracked metallic structures has benefited due to the increasing demand for life extension of both military and civil aircrafts leading to significant advances in repair technology of damaged metallic structures, thus, proving bonded composite repairs of metallic structures a rapidly growing technology in the field of aerospace. Given the specific characteristics of a bonded composite repair and the differences in the materials used in each case (metal, composite & adhesive), the applicability of a number of Non Destructive Testing (NDT) methods to trace crack propagation under a composite patch repair is investigated, following fatigue testing. For this scientific venture, the main NDT methods examined include Bragg grating optical sensors (embedded into composite patches) as well as the eddy current method applied over a bonded composite repair (i.e. avoiding repair disassembly). Bragg grating sensors were proven capable of tracing crack propagation with high accuracy, through interpretation of the differences caused in the strain field over the crack, after comparison with finite element analysis results. On the other hand, the capability and the reliability of the eddy-current method to detect cracks under a composite obstacle of significant thickness were checked over a range of patch thicknesses. The eddy-current method was found to be fully capable of tracing the crack propagation under the composite patch, requiring only proper calibration of the generator. Minute differences in crack lengths between the patched and the unrepaired side of the specimen examined were due to their non-symmetric configuration, which induced different stress intensity factors at the patched and the unrepaired sides, as finite element analysis has shown.

Keywords: Bonded Composite Repair, Bragg Gratings, Eddy-Current, Non Destructive Testing.

1. INTRODUCTION

The economic world conditions are forcing to the operation of aircrafts well beyond their original design life, resulting in innovative repair techniques. As a result, the adhesively bonded composite patch repair of metallic aircraft components is becoming an established technology. Bonded repairs are mechanically efficient, cost effective and can be applied rapidly to produce an inspectable damage tolerant repair. Compared to metals, advanced fiber composites have the advantages of formability, tailorability of stiffness, high specific strength and immunity to corrosion and fatigue. Composite patches can be pre-cured and secondarily bonded on cracked structures or cocured in situ. The greatest concerns with mechanical repairs are the danger of crack initiation from one of the new fastener holes, as well as the difficulty in detecting this crack by standard Non Destructive Testing (NDT) procedures, until the crack emerges from under the repair. On the other hand, the bonded patch, if correctly designed, has a relatively small influence on the stress field, so no crack initiation occurs in adjacent regions [1-6].

One of the most significant advantages of the boron composite patches is the ability to trace crack propagation in its early stages, when the crack tip is still under the composite patch, using standard NDT procedures, such as the eddy-current method. This is due to the inherent characteristics of the boron fibers, thus enabling the application of the eddy-current method. In this paper, the eddy current method applied over a bonded composite repair (i.e. without removing the repair) to verify the capability and the reliability of the method to detect cracks under a composite obstacle of significant thickness is examined for several patch thickness.

Additionally, in order to enable on line monitoring of the local stress field into a composite patch during the expected crack propagation, optical fiber sensors can be structurally integrated into it. Fiber optic sensors present significant advantages, compared to other techniques in the area of stress-strain monitoring (e.g. strain gages, etc.), mainly concerning their extremely small size, the resistance to corrosion and fatigue, their immunity to electrical interference, as well as their chemical and mechanical compatibility with composite materials. In this paper, the capability of the optical fiber Bragg Grating sensors is verified to monitor both the crack propagation in the metal, as well as the propagating adhesive debonding due to mechanical or thermal fatigue.

2. BRAGG GRATING OPTICAL SENSORS

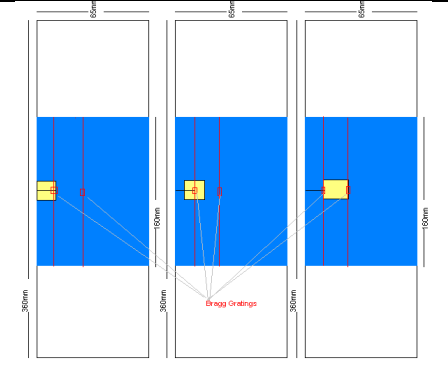
In the present study, Fiber Bragg grating sensors were embedded in the composite patches, to trace the mechanical field variations. The field variations, for simplicity reasons, were assumed mechanical only, decoupled from any thermal effect, by keeping the environmental conditions stable during the experimental study. Various specimens were designed and manufactured. First of all, the behavior and the repeatability of the strain measurements taken from the Bragg sensors were evaluated together with the durability of the sensor during the test process. The materials used for the manufacturing of the specimens (Type I specimens) are presented in Table I. The vertical projection of the crack tip of the metallic structure was chosen as the sensor location, based on the numerical simulation results presented in [7]-[11]. The composite patch was manufactured using six laminates of carbon epoxy prepreg. The sensor was embedded between the third and fourth lamina, based on the results of [10]. The specimens were gradually loaded to a range of 1 to 10 KN tensile load and measurements for each load

condition were recorded from the optical fiber sensors. A Micron Optics Bragg Gratings Interrogator has been used for the acquisition of measurements, having the capability to store digitally the wavelength shifts of the sensors during the loading process.

Additional specimens were manufactured in order to study potential adhesive debonding propagation (Type II specimens). Each of these specimens was representing a potential debonding (yellow area in picture included in Table II) developed in the area of the crack tip, between the composite patch and the repaired metallic area. The aim of the test series was to examine the possible propagation patterns of the cracked and/or debonding area, using NDI techniques. The specimens, manufactured using Table II materials with six ply composite patch, were submitted to fatigue testing at Mean load 2.1 tn, Amplitude 1,9 tn and Load frequency of 10 Hz. Finally, in order to monitor the propagation of a crack in a composite patch repair, more specimens were manufactured, having two embedded optical fiber sensors (Type Iii specimens). The crack tip sensor was called as sensor “a” while the second sensor was called “b”. The loading conditions of the specimens were identical with the previous ones. The data acquisition during the fatigue loading of these specimens included measurement of crack length at 10K cycles and every 2.5K cycles with simultaneous sensor wavelength shift recording, measurement of debond area using C-Scan NDI every 10K cycles and ramp type tensile loading every 10K cycles with simultaneous sensor wavelength shift recording

Table I: Material properties and basic specimen's geometry

| Material | Thickness (mm) | E (MPa) | G (MPa) | ν |
|----------------------|------------------|---------|---------|-------|
| Aluminium 2024-T3 | 6 | 72000 | 26900 | 0.3 |
| Textron 5521 Prepreg | 0.125 per lamina | 207000 | 4800 | 0.21 |
| FM73 Film Adhesive | 0.2 | --- | 750 | --- |
| Optical Fiber | Diameter 0,1mm | 70000 | | 0.29 |



The results of the tensile loading of specimens type I are presented in the left part of Figure 1. It is shown that the repeatability of measurements is very satisfying and the strain measuring capability of the sensor is accurate, therefore the sensors were considered appropriate for the experiment.

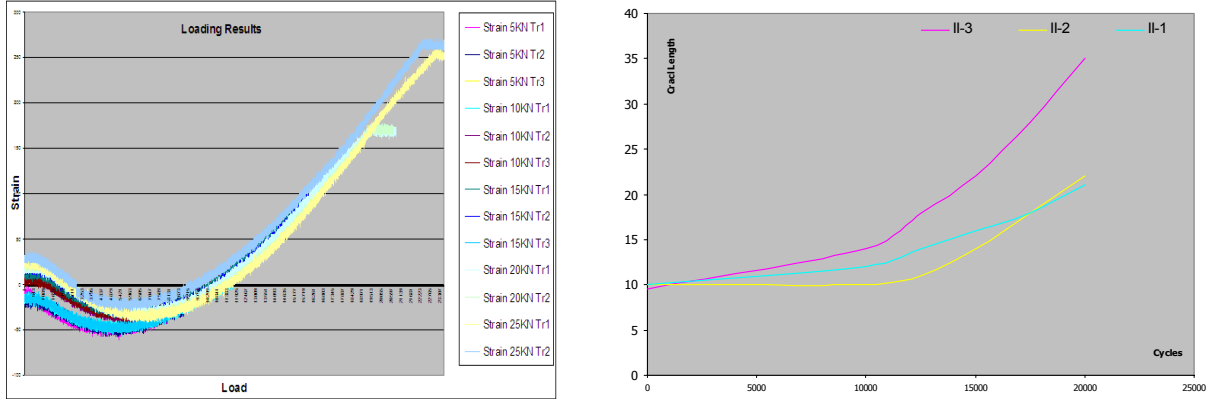


Figure 1: Load vs. Strain results during repeatability test (left) and crack extension of specimens Type II (right)

It was also found that during the initial tensile loading, compressive loads are developed near the crack tip, due to the fact that the specimen has a resulted curvature from the curing process because of the thermal coefficient mismatch of the patch and the aluminum material. Representative results of the specimen type II loading, with respect to crack extension, are presented in the right part of Figure 1. Moreover, C-Scan NDI was performed on these specimens in order to check the debond propagation due to the fatigue loading. Various results were taken from the fiber optic sensors during the testing of specimens type III. The results are split in two major categories: results related to the debond extension and results related to the crack propagation. Some representative results concerning bond extension monitoring, are presented in Figure 2. From the above results it is obvious that, during the ramp loading, there is a shift in strain measurement due to the fact that the debond has propagated and resulted in a field alternation near the fiber optic sensors.

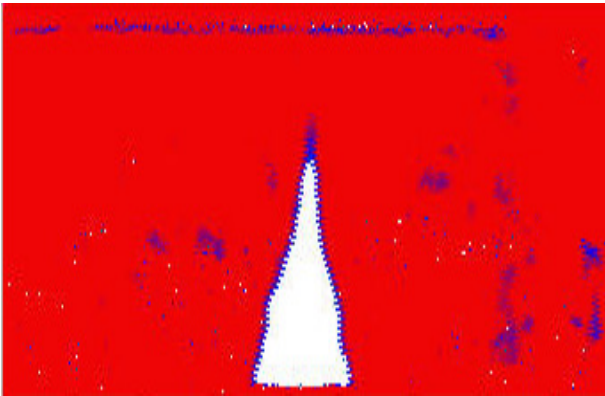
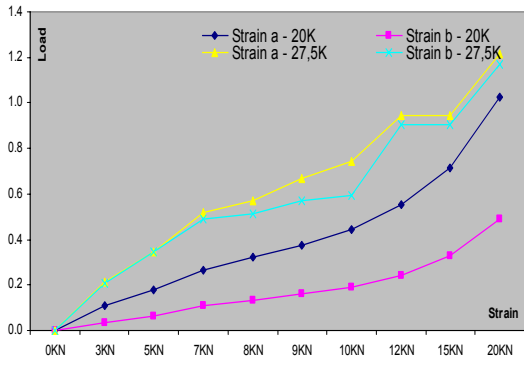


Figure 2: Debonding extension monitoring and final debonding area for specimens Type III.

Some representative results concerning the crack propagation monitoring, are presented in Figure 3. From the above results, a strain increment is obvious during the crack propagation. Moreover, for the sensor “b” of each specimen, a sudden strain increment was noticed when the crack was passing through the vertical level of the sensor. Moreover, according to further processing of the results, it was noticed that during the crack propagation and when the crack “passes” from the sensor “b”, the increment curves of the two sensors cross each other, giving a notion of the crack length on that time. More details on the experimental process followed together with analytical results can be found in [12].

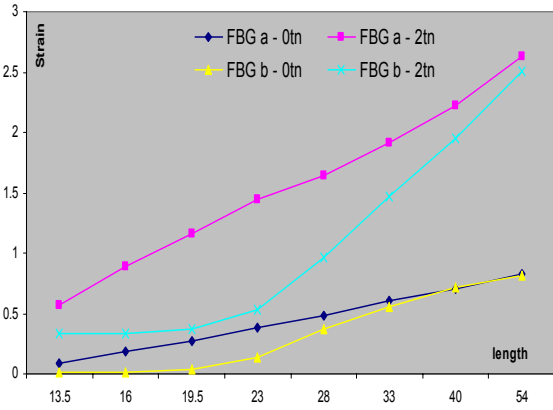
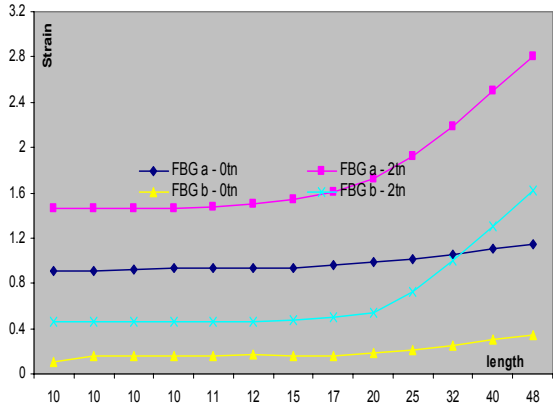


Figure 3: Representative crack propagation monitoring results

3. EDDY CURRENT

Notched specimens were fabricated using Aluminum and Boron Epoxy patches were bonded using film adhesive to the one side of the metallic specimens. Further propagation of the initial cracks was achieved by fatigue loads. Accuracy of the eddy-current method was verified by measuring the crack lengths on both sides of the specimen and comparing the results, while the eddy-current generator calibration parameters according to the patch thickness have been recorded.

The selection of the specimen configuration as well as the choice of the materials from which the specimens would be fabricated for this paper were driven by the cases of repairs usually met in the field of aeronautics technology, where composite patch repairs are usually applied. As a result, relatively thin (only 6mm thick) specimens made of Aluminum 2024-T3 were fabricated, representing an external aircraft's skin. The dimensions of the specimens were 360x65 mm, while 10mm notches were induced to them in order to enable crack initiation after fatigue loading. The Boron Epoxy patches were pre-fabricated in an autoclave using 5521 Textron prepreg. All the composite patches were unidirectional, which is the case met in most actual repairs, in order to coincide with primary loading direction. Their dimensions were 160x65 mm, in order to cover the full notch length and to enable further propagation of the crack under them, while their thickness was from 2 layers (0.25mm) to 7 layers (0.875mm) to represent actual structural composite patch repairs. Composite patches were bonded over the cracked metallic specimens using FM73 high performance film adhesive. The metallic specimens were initially surface treated to ensure a reliable bonding of the patch over the specimen. Surface treatment included grit blasting as well as silane. The adhesive was cured at 120° C for 1 hour to achieve the specified strength of the bonding.

The specimens were loaded by means of an INSTRON 8501 fatigue loading machine. Tension – tension loads between 2000N and 60000N (corresponding to 154MPa maximum remote stress) was applied to all specimens with 1Hz frequency. Minimum load was chosen to be slightly higher than zero in order to avoid possible compression loading because of late response of the machine control unit or from inertia effects.

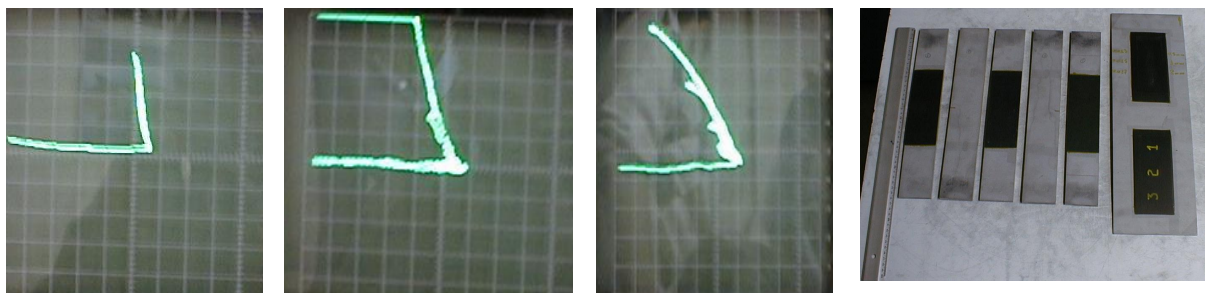


Figure 4: *Waveform produced by the crack measured at the unpatched (1st photo) and the patched side (2nd photo) measured above the boron patch. Waveform produced by the three different cracks (0.5mm, 1mm and 2mm) above the boron patch of the calibration specimen (3rd photo). Specimens manufactured and calibration specimen (4th photo)*

After the fatigue loading process NDI was performed by means of an NORTEC NDT-25L eddy current generator, using a 100Hz probe. Crack lengths were calculated by measuring the distance between the point which the eddy-current method indicated as crack tip and the edge of the specimen. Initially the instrument was calibrated for the NDI of the unpatched sides,

using an angle of 283° , Gain=48 (24dB), Filter=0, Vsensitivity=0.2 and Hsensitivity=1. The waveform produced because of the cracks is shown in Figure 4, while the measured crack lengths are presented in Table II. The calibration of the instrument for the NDI above the boron patch was achieved by using a patched aluminum plate with cracks of known length under it. The produced waveform for the different crack lengths (0.5mm, 1mm and 2mm) is shown in the 3rd picture of Figure 4. The angle varied according to the number of layers of the patch (226° for 2 layers, 223° for 4 layers and 219° for 7 layers) while the rest of the parameters were kept to their original values.

Table II: Experimental and numerical results

| Specimen Number | Patch Thickness (mm) | Out-of-plane Displacement FEA (mm) | Out-of-plane Displacement Experimenta I (mm) | Stress Intensity Factor Patched Side | Stress Intensity Factor Unpatched Side | Crack length Patched Side (mm) | Crack length Unpatched Side (mm) | Number of Cycles |
|-----------------|----------------------|------------------------------------|--|--------------------------------------|--|--------------------------------|----------------------------------|------------------|
| 1 | 0.25 | 0.64 | 0.56 | 684.2 | 1309.4 | 20 | 22 | 11000 |
| 2 | 0.25 | 0.64 | 0.56 | 684.2 | 1309.4 | 20 | 22 | 7500 |
| 3 | 0.50 | 0.92 | 1.01 | 626.8 | 1315.1 | 22 | 27 | 11000 |
| 4 | 0.50 | 0.92 | 1.075 | 626.8 | 1315.1 | 22 | 27 | 8000 |
| 5 | 0.875 | 1.18 | 1.26 | 589.9 | 1318.3 | 22 | 24 | 10500 |

The crack lengths measured above the patch were compared with the corresponding crack lengths measured from the non-patched side of the specimen. As obviously shown in Table II, the crack lengths at the unpatched side were slightly higher than the ones measured at the patched side. Again, this was predicted from the finite elements analysis, by the different values of the stress intensity factor at the two sides of the specimen, which resulted in different crack propagation rates. In Figure 5 a detail of the mesh in the crack area is presented together with some FEA results, which provide a qualitative explanation concerning the difference in the crack propagation rates between the unpatched and the patched side of the specimen. More details on the experimental process followed together with analytical results can be found in [7].

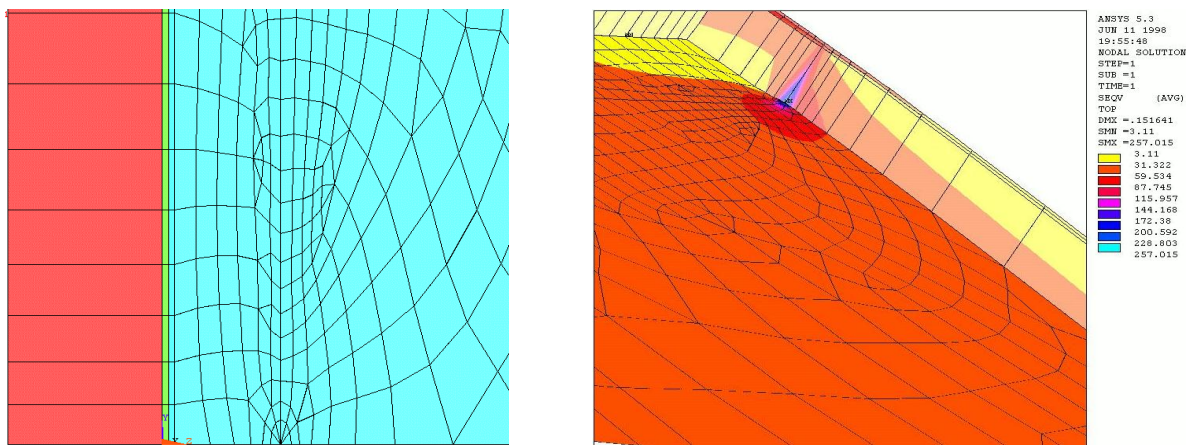


Figure 5: Detail of the different layers and the crack area (left) and qualitative FEA results explaining the difference in the crack propagation rates between the unpatched and the patched side of the specimen.

4. CONCLUSIONS

According to the theoretical and experimental results described in this paper, the eddy-current method was found to be fully capable of tracing the crack propagation under the composite patch, requiring only proper calibration of the generator. Small differences in the crack lengths between the patched and the unpatched side of the specimen which were examined were explained by their non-symmetric configuration, which induced different stress intensity factors at the patched and the unpatched sides, as finite element analysis has clearly shown. As far as the embedding of fiber Bragg grating sensors is concerned, it was found out that optical fiber sensors can be used efficiently to monitor the health of a composite patch repaired structure. The sensors presented very good measurement stability, great sensitivity and the capability to trace effectively propagating failures in the repaired area.

REFERENCES

- [1] A. A. Baker, Bonded Composite Repair of Metallic Aircraft Components – Overview of Australian Activities, AGARD, CP-550.
- [2] Z. P. Marioli-Riga, G.J. Tsamasphyros, G.N. Kanderakis, Development of a Method for A/C Emergency Repairs by Composite Patches, S.A. Paipetis, E.E. Gdoutos, (Xanthi1997), Vol II 143-156
- [3] C. N. Duong, Yu J., The Stress Intensity Factor for a Cracked Stiffened Sheet Repaired with an Adhesively Bonded Composite Patch, International Journal of Fracture 84(1997), p. 37-60
- [4] A. A. Baker, R. Jones, Bonded Repair of Aircraft Structures, Martinus Nijhoff Publishers, Dordrecht, (1988).
- [5] Composite Repairs of Cracked Metallic Airframe Structures, U.S. Department of Transportation, Federal Aviation Administration, CT-92/32 (May 1993).
- [6] G. J. Tsamasphyros, G.N. Kanderakis, Z.P. Marioli-Riga, Three-dimensional Finite Elements Analysis of Debonding and Thermal Effects Near the Crack-Tip of a Metal Structure Repaired by a Composite Patch, 5th National Congress on Mechanics, University of Thessaly, Greece, June 1999.
- [7] [8] G. J. Tsamasphyros, G. N. Kanderakis, N.K. Furnarakis, Z. P. Marioli-Riga, Optimization of Embedded Optical Sensor Locations in Composite Repairs Applied Composite Materials Volume 10 No3: 129-140, May 2003, Kluwer Academic Publishers, Netherlands.
- [8] G. J. Tsamasphyros, N.K. Furnarakis, G.N. Kanderakis, Three Dimensional Finite Element Analysis of Composite Patches with Embedded Optical Fibres – Through Thickness Optimization, Z. P. Marioli-Riga “International Conference on Computational Engineering & Sciences, ICES’01, Puerto Vallarta, Mexico (2001).
- [9] G. J. Tsamasphyros, G. N. Kanderakis, N. K. Furnarakis, Z. P. Marioli-Riga, R. Chemama, R. Bartolo, Three – Dimensional Finite Element Analysis of composite patches with embedded optical fibers – Selection of Optical Fibers Paths and Sensors Locations, Structural Health Monitoring 2002, Daniel L. Balageas, 1203-1210, Destech Publications, ENS Cachan France, July 10-12, 2002.
- [10] G. J. Tsamasphyros, N. K. Furnarakis, G. N. Kanderakis, Z. P. Marioli-Riga, Three – Dimensional Finite Element Analysis of composite patches with embedded optical fibers – Optimizing Optical Fiber Embedding Location: Structural Health Monitoring

- 2002, Daniel L. Balageas, 1219-1226, Destech Publications, ENS Cachan France, July 10-12, 2002.
- [11] G. J. Tsamasphyros, G. N. Kanderakis, N. K. Fournarakis, Z. P. Marioli-Riga, Detection of patch debonding in composite repaired cracked metallic specimens, using optical fibers and sensors SPIE Optical Metrology Conference, 23-26 June 2003, Munich, Germany.
- [12] Z. P. Marioli Riga, A. Karanika, S. Panagiotopoulos, G. J. Tsamasphyros, G. N. Kanderakis, N. K. Furnarakis, Structural Health Monitoring of composite patch repairs using embedded fiber bragg grating sensors, 5th GRACM International Congress on Computational Mechanics, Limassol, Cyprus, 29 June – 1 July 2005, Edited by G. Georgiou, P. Papanastasiou and M. Papadrakakis, pp.687-694.
- [13] Z. P. Marioli-Riga, G.J. Tsamasphyros, G.N. Kanderakis, Non Destructive Evaluation of the Crack Propagation under a Composite Patch Repair Using the Eddy Current Method, “The International Society for Optical Engineering” (SPIE), Newport Beach, CA, USA (2000).